

Cosmology meets functional QCD: First-order cosmic QCD transition induced by large lepton asymmetries

Fei Gao^{1,*} and Isabel M. Oldengott^{2,3,†}

¹*Institut für Theoretische Physik, Universität Heidelberg, Philosophenweg 16, 69120 Heidelberg, Germany*

²*Centre for Cosmology, Particle Physics and Phenomenology,
Université catholique de Louvain, Louvain-la-Neuve B-1348, Belgium*

³*Departament de Física Teòrica and IFIC, CSIC-Universitat de València, 46100 Burjassot, Spain*

(Dated: January 4, 2022)

The lepton flavour asymmetries of the Universe are observationally almost unconstrained before the onset of neutrino oscillations. We calculate the cosmic trajectory during the cosmic QCD epoch in the presence of large lepton flavour asymmetries. By including QCD thermodynamic quantities derived from functional QCD methods in our calculation our work reveals for the first time the possibility of a first-order cosmic QCD transition. We specify the required values of the lepton flavour asymmetries for which a first-order transition occurs for a number of different benchmark scenarios.

PACS numbers: 95.30.Tg, 11.30.Fs, 05.70.Jk, 12.38.Lg

Keywords: cosmic QCD transition, lepton asymmetry, functional QCD

Introduction According to the hot big bang model, the early Universe has experienced (at least) two epochs where phase transitions could occur: the electroweak transition at temperatures around $T_{ew} \sim 100$ GeV when fermions and gauge bosons became massive particles; and the transition of quantum chromo dynamics (QCD) at $T_{QCD} \sim 130$ MeV when quarks confined into hadrons. After the recent (direct) discovery of gravitational waves (GWs) by LIGO [1] the interest in phase transitions in the early Universe has experienced a revival. First-order transitions are typically accompanied by processes that emit GWs while crossovers do not lead to a strong enhancement over the primordial GW spectrum. The perspective of measuring GWs therefore opens up a new window to the early Universe and a means to explore new physics.

The Standard Model (SM) of particle physics predicts both the electroweak as well as the QCD transition to be crossovers. However, a couple of observations from cosmology and particle physics unavoidably hint towards the existence of physics beyond the SM. The phenomenon of dark matter, the value of the matter-antimatter asymmetry of the Universe and the observation of neutrino oscillations are arguably the most unambiguous evidences thereof. Many extensions of the SM would render the electroweak transition to be first-order (for the most simple extension see [2]), while there are much fewer mechanisms known that could provide a first-order QCD transition ([3, 4]). Besides the emission of GWs, a first-order QCD transition could lead to the production of exotic relics [5, 6]. The details of the QCD transition – either first-order or crossover – furthermore have an impact on the production of primordial black holes [7–11] which are one of the prime candidates for dark matter.

In this work, we show for the first time that large lepton flavour asymmetries can render the QCD tran-

sition to be first-order. The fact that the value of lepton asymmetry has an impact on the cosmic QCD epoch has already been known for a while and been discussed in a series of papers [12–14]. However, so far it has not been possible to provide a definite answer to the question whether a sufficiently large lepton asymmetry can indeed render the transition to be first-order and what *sufficiently large* means quantitatively. This is to some extent due to the restricted range of applicability of the Taylor expansion of the QCD pressure in [13, 14]. To consistently describe the cosmic trajectory in different regions of the QCD phase diagram from crossover to first-order phase transition, the complete phase structure and the related thermal properties in a large range of temperature and chemical potential are required. Therefore, in this work, we take a different approach: Instead of relying on a Taylor expansion we include results from functional QCD methods [15, 16] into our calculations of the cosmic trajectory at the QCD epoch.

QCD diagram QCD matter experiences a transition from quarks and gluons to hadrons as temperature and chemical potential changes. To chart the phase diagram of QCD for non-zero temperature, charge- and baryon chemical potential has attracted a lot of interest. Theoretical studies have confirmed a crossover at zero chemical potential [17], while the region of a first-order phase transition at large chemical potential is still not fully settled. Most of the theoretical studies using effective models or certain truncations have observed the existence of the critical end point (CEP), but the determination of its location is still work in progress as it varies in different computations. Searching for signals of the QCD phase transition, especially the CEP, are the main goals of the current and the future experimental program at the relativistic heavy ion collider [18–21].

Lattice QCD simulations have depicted solid compu-

tations at vanishing chemical potential [22–24]. However, due to the sign problem, it is difficult for lattice QCD to reach large chemical potentials. Large chemical potentials are accessible by continuum QCD methods, i.e. functional QCD methods including Dyson-Schwinger equations (DSEs)[25–28] and the functional renormalization group (fRG) method [29, 30]. The functional QCD methods are non-perturbative continuum methods which are capable of describing both the dynamical chiral symmetry breaking (DCSB) and the confinement simultaneously. Though limited by the truncations, the functional QCD approaches have made fruitful progress in studying the QCD phase structure and thermal properties [28, 31–33]. The approaches have delivered a complete phase diagram and also related thermal properties in a large range of chemical potential which could serve as guidelines for exploring QCD features.

Large Lepton Asymmetry When the Universe expands and cools down it follows a certain path in the QCD phase diagram, the so called *cosmic trajectory*. The standard cosmic trajectory is based on the assumption that matter and antimatter are (almost) equally abundant in the Universe. Indeed, measurements of primordial element abundances and the anisotropy spectrum of the CMB show that the Universe only has a tiny asymmetry in the baryonic sector, characterized by the *baryon asymmetry* $b = (8.7 \pm 0.06) \times 10^{-11}$ (inferred from [34] and where b is going to be properly defined in eq. (2)). This tiny number is however still many orders of magnitude larger than predicted by the SM and necessitates theories of baryogenesis and leptogenesis. The idea of leptogenesis is to create an asymmetry in the leptonic sector and transfer this lepton asymmetry into a baryon asymmetry by sphaleron processes. According to this idea the lepton asymmetry would be of the same order of magnitude as the baryon asymmetry, or more explicitly $l = -\frac{51}{28}b$ [35]. If the lepton asymmetry is indeed as tiny as the baryon asymmetry this implies that the cosmic trajectory passes the QCD diagram at (extremely) small chemical potential where lattice calculations reveal a crossover. Observational constraints from big bang nucleosynthesis (BBN) [36] and the CMB [37] on the value of the lepton asymmetry however allow values of the lepton asymmetry as large as $|l| < 1.2 \times 10^{-2}$ [37], i.e. around 8–9 orders of magnitude larger than the baryon asymmetry. From a theoretical point of view, there are also alternative models which predict a large lepton asymmetry [38–41].

Observationally even less constrained than the *total* lepton asymmetry $l \equiv l_e + l_\mu + l_\tau$ are the individual lepton flavour asymmetries $l_{\alpha=e,\mu,\tau}$: It has been shown [42, 43] that initially different lepton flavour asymmetries are equilibrated at around $T_{osc} \sim 10$ MeV when neutrino oscillations become efficient such that finally $l_\alpha \approx \frac{1}{3}$ [44]. This implies that CMB and BBN constraints are only sensitive to the value of the total lepton asymme-

try l but have no constraining power on the initial values of the individual lepton flavour asymmetries l_α . From an agnostic point of view, the individual lepton flavour asymmetries should therefore be treated as free parameters (while their sum still needs to fulfill the observational constraint $|l| < 1.2 \times 10^{-2}$ [37]). In any case, lepton asymmetry is a key parameter to understand the origin of the matter-antimatter asymmetry of our Universe. As it will become clear in the following, a large lepton asymmetry would shift the cosmic trajectory towards large chemical potentials and therefore possibly impact the nature of the cosmic QCD transition.

Cosmic trajectory Let us in the following explain how we calculate the cosmic trajectory. The basic idea of the method is similar to the one outlined in [12–14].

Within the framework of the SM, before the onset of neutrino oscillations at $T_{osc} \approx 10$ MeV and after the electroweak transition at $T_{ew} \approx 100$ GeV electric charge, baryon number and lepton flavours are conserved in a comoving volume. Assuming as well entropy conservation in comoving volume, the baryon number b , lepton flavour number l_α and electric charge q in comoving volume can be written as

$$l_\alpha = \frac{n_\alpha + n_{\nu_\alpha}}{s} \quad (\alpha = e, \mu, \tau), \quad (1)$$

$$b = \sum_i \frac{B_i n_i}{s}, \quad (2)$$

$$q = \sum_i \frac{Q_i n_i}{s}, \quad (3)$$

and *remain constant* throughout the evolution of the Universe, for temperatures $T_{ew} > T > T_{osc}$. The sum in eq. (2) goes over all baryons and in eq. (3) over all charged particles. n_i denotes the net number density (i.e. particle minus anti-particle number density) of particle species i and s denotes the total entropy density. In the following we will refer to l_α , b and q as lepton flavour, baryon and charge asymmetry. As mentioned above, the baryon asymmetry is a known quantity and we fix it to the central value $b = 8.7 \times 10^{-11}$ from [34]. There is furthermore good reason to believe that the Universe is charge neutral [45] such that we may set $q = 0$ from now on. While the standard assumption is $|l_\alpha| = \mathcal{O}(b)$ we treat the three lepton flavour asymmetries l_α as free input parameters (within observational constraints). This may be realized by some new physics violating lepton flavour around some temperature T_{BSM} after the electroweak epoch but well before the QCD epoch, such that the l_α in eq. (1) are conserved at $T_{BSM} > T > T_{osc}$. The net number densities n_i are understood to be functions of temperature T_i and chemical potential μ_i . We assume kinetic equilibrium, i.e. all particles sharing the same temperature $T_i = T$, and chemical equilibrium which allows us to find relations between the chemical potentials of differ-

ent particle species, e.g. $\mu_u = \mu_c$ etc. Furthermore, each conserved charge is associated with a chemical potential (i. e. μ_B, μ_Q and μ_{L_α}), which can be related to the chemical potentials of the different particle species by (see also [12])

$$\mu_{L_\alpha} = \mu_{\nu_\alpha}, \quad (4)$$

$$\mu_Q = \mu_u - \mu_d, \quad (5)$$

$$\mu_B = \mu_u + 2\mu_d. \quad (6)$$

The cosmic trajectory denotes the solution of eqs. (1) – (3) for $(\mu_{L_\alpha}, \mu_B, \mu_Q)$ at different temperatures T and given a choice for the lepton flavour asymmetries l_α . As first noted in [12], the cosmic trajectory shifts towards larger values of $(|\mu_{L_\alpha}|, |\mu_B|, |\mu_Q|)$ for increasing values of $|l_\alpha|$. Qualitatively this can be understood in the following way: Large values of l_α imply large corresponding lepton chemical potentials, through eq. (1). On the other hand, keeping $q = 0$ fixed in eq. (3) induces large chemical potentials for the quarks such that they can compensate for the asymmetry in the charged lepton sector. Through eqs. (5) and (6) it therefore becomes clear that large lepton asymmetries l_α do not only imply large leptochemical potentials μ_{L_α} but also large charge- and baryon chemical potentials.

In practice, in order to solve eqs. (1)-(3) we need to make assumptions about the thermodynamic quantities of the different particle species, i.e. about the number densities n_i and the entropy density s . For leptons and photons we assume Fermi-Dirac or respectively Bose-Einstein distributions for the phase-space densities, in accordance with the assumption of thermal and chemical equilibrium. Number and entropy densities are then simply obtained by momentum integration. Concerning the DCSB and confinement phenomena, modelling the QCD sector at temperatures close to the QCD transition is however much more complicated.

Let us briefly summarize the approach of [13, 14] before we explain how we treat the QCD particle content in this work. In [13, 14] the QCD sector was treated separately in three different (but overlapping) temperature regimes [46]: i) at high temperatures quarks and gluons were treated as free particles, i.e. assuming Fermi-Dirac or respectively Bose-Einstein equations, where [14] also included contributions from perturbative QCD, ii) at temperatures around the QCD transition the QCD pressure was Taylor expanded and susceptibilities from lattice QCD were used in order to describe thermodynamic quantities, iii) at low temperatures QCD matter was described by the hadron resonance gas (HRG) model, i.e. by assuming thermal distributions for hadrons. The trajectories derived within the different temperature regimes turned out to be relatively smoothly connected. As pointed out in [14], the method however has two limitations. The appearance of a Bose-Einstein condensate of pions for large lepton asymmetries (see also [10]) would

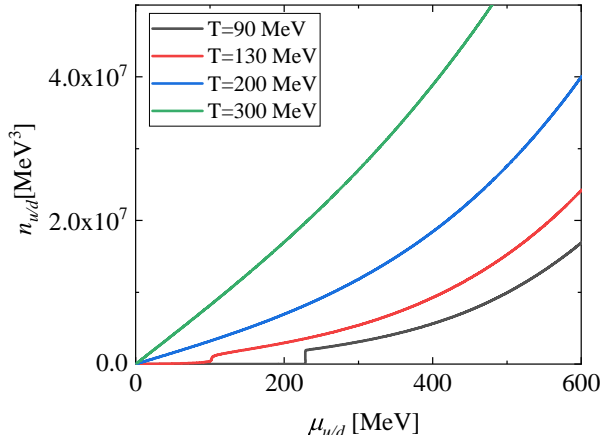


FIG. 1. Number densities of the u/d quark as a function of the chemical potential and for different temperatures in crossover and first-order phase transition region.

require a separate treatment of the low-energy modes of pions. The more stringent restriction however comes from the application of the Taylor expansion of the QCD pressure which is only justified for relatively small chemical potentials.

In this work, we therefore apply the thermodynamic quantities derived from Dyson-Schwinger equations in the rainbow-ladder(RL) truncation. Fig. 1 shows the number density $n_{u/d}$ of the u/d quark as a function of their chemical potential $\mu_{u/d}$ and for different values of the temperature T . Observe that for temperature below $T = 130$ MeV (red) a sudden drop in the number density appears. This discontinuity displays a first-order phase transition and the temperature and chemical potential above which it appears marks the critical end point $(T_{\text{CEP}}, \mu_{\text{CEP}})_{u/d}$. Closer investigation shows that $(T_{\text{CEP}}, \mu_{\text{CEP}})_{u/d} = (125, 111)$ MeV [15]. In general the heavier quarks have a different CEP, expected to lie at larger chemical potential due to the larger masses. Note that the number density in fig. 1 is not based on any assumption about the thermodynamic processes nor does it know about any conservation laws. It can be applied to different physical scenarios (e.g. heavy ion collisions or cosmology) by imposing additional constraints, as in our case eqs. (1)-(3). The access to the first-order phase transition allows us to consistently explore the Universe's evolution across different regions of the QCD phase diagram. Let us however note here that rather than being able to determine the exact location of the CEP the strength of the RL truncation is to capture the main properties of the QCD phase structure. Therefore, our work should also be understood as a *proof-of-principle of the possibility of a first-order cosmic QCD* induced by large lepton flavour asymmetries – and not as a method enabling the exact determination of cosmic trajectories

during the QCD epoch.

Method The required thermal properties, number density and entropy density, can be computed after solving the quark gap equation of DSEs [15, 47, 48]. We here apply the same settings for the gap equation as described in Ref. [15], and then solve it through Broyden's iteration method in Fortran.

The number density for u/d, s and c quarks can be directly computed from the solution of the quark gap equation after subtraction, i.e. through the quark propagator G ,

$$n(T, \mu) = - \int \frac{d^3 \vec{p}}{(2\pi)^3} \left\{ T \sum - \int \frac{dq_0}{2\pi} \right\} (\text{tr}[\gamma_0 G]). \quad (7)$$

The entropy density can then be expressed as the integral along the chemical potential as

$$\delta s(T, \mu) = s(T, \mu) - s(T, \mu = 0) = \int_0^\mu \frac{\partial n(T, \mu)}{\partial T} d\mu. \quad (8)$$

Due to the lack of gluon pressure in the approach of Ref. [15], we here use the lattice QCD computation at zero chemical potential with $N_f = 2 + 1 + 1$ as parametrized in Ref. [49]. The full entropy is given as:

$$s_{\text{QCD}} = s_{\text{latt}}(T, \mu = 0) + \delta s(T, \mu). \quad (9)$$

The data of the number density and the entropy density are then generated on a grid of values for temperature and chemical potential. The grid spans over the temperature range $T = 121 - 400$ MeV, where we chose a grid size of 1 MeV at $T < 140$ MeV, a grid size of 5 MeV a $140 < T < 300$ MeV and a sparse grid size of 20 MeV at $300 < T < 400$ MeV. Even though the data for $T < 121$ MeV are available, the truncation has been much less reliable in this regime. The number density below $T < 120$ MeV gives an odd rising behaviour as T decreases, which can possibly be solved by improving the truncation. Nevertheless, the temperature range we chose still covers the CEP and first-order phase transition region. The pion condensation effect on the quark propagator is not included in the current truncation. Such an effect is in the hadron resonance channel of quark gluon vertex which is the subleading contribution [16], and hence will barely have impact on the QCD transition. In some certain cases, the pion condensation phase transition and QCD transition can take place successively. In μ -direction the grid spans over the range $0 < \mu < 1000$ MeV, with a uniform grid size of 1 MeV. Both number densities and entropy densities of the different particle species were stored in data files.

In order to calculate the cosmic trajectory we modified the c-code developed in [12–14] such that it reads in those data files and interpolates them. The code uses Broyden's method in order to find solutions of eqs. (1)-(3) for $(\mu_{L_e}, \mu_{L_\mu}, \mu_{L_\tau}, \mu_B, \mu_Q)$, given the above specified temperature values and with l_α as input parameters. In

order to interpolate the data for number and entropy density in μ -direction we applied cubic spline interpolation.

Results Throughout this work, we focus on the following choices for lepton asymmetries l_α during the QCD epoch:

- (i) $l_e = l_\mu = l_\tau = \frac{l}{3}$ (equilibrated case),
- (ii) $l_e = 0, l_\mu = -l_\tau$,
- (iii) $l_e = -l_\tau, l_\mu = 0$,
- (iv) $l_e = -l_\mu, l_\tau = 0$,
- (v) $l_e = l_\mu, l_\tau = -2l_e$,
- (vi) $l_e = l_\tau, l_\mu = -2l_e$,
- (vii) $l_e = -2l_\mu, l_\mu = l_\tau$.

As noted before, case (i) is constrained by CMB observations to values $|l| < 1.2 \times 10^{-2}$ [37]. Cases (ii)-(vii) were chosen such that the total lepton asymmetry l always fulfills the CMB constraints. Note that there is of course an infinite number of realizations for scenarios with $l_e \neq l_\mu \neq l_\tau$ satisfying the CMB and BBN constraints. Scenarios (ii)-(vii) simply serve as benchmark models.

The main question we are interested in is whether large lepton flavour asymmetries can indeed render the cosmic QCD transition first-order, as it has been speculated in [12–14]. Answering this question does not even require to solve eqs. (1)-(3) for the whole temperature range. It suffices to work out if at $T = T_{\text{CEP}}$ we find either $\mu_u \geq \mu_{\text{CEP}}$ or $\mu_d \geq \mu_{\text{CEP}}$ (or both). s and c quark can generally also experience a first-order transition but since their critical end point is expected to be at larger chemical potentials we expect this to happen for larger l_α . We therefore concentrate on the u and d quark in the following. To quantify for which value of l_α a first-order transition may happen we add

$$\mu_i \geq 111 \text{ MeV} \quad \text{at } T = 125 \text{ MeV} \quad (10)$$

as an additional equation on top of eqs. (1)-(3), where i is equal to *either* u *or* d . This additional constraint eliminates one degree of freedom. While the calculation of the cosmic trajectory usually treats the three l_α values as free input parameters, for the problem at hand only two l_α are free, the third one is determined by solving eqs. (1)-(3) at $T = 125$ MeV plus eq. (10). Since all cases (i)-(vii) considered in this work are characterized by only one degree of freedom, no further input is required.

The first result of this work is the fact that there exist solutions for the set of equations, i.e. for large enough lepton asymmetries *the Universe experienced a first-order QCD transition*. Table I summarizes for which values of the lepton flavour asymmetries either the u or the d quark experiences a first-order phase transition. For

	$\mu_u \geq 111 \text{ MeV}$	$\mu_d \geq 111 \text{ MeV}$
(i)	$l \geq 1.10 \times 10^{-1}$	$l \leq -1.03 \times 10^{-1}$
(ii)	$l_\mu \geq 7.43 \times 10^{-2}$	$l_\mu \leq -6.85 \times 10^{-2}$
(iii)	$l_e \geq 7.14 \times 10^{-2}$	$l_e \leq -6.59 \times 10^{-2}$
(iv)	$l_e \geq 1.36 \times 10^{-3}$	no solution
(v)	$l_e \geq 3.46 \times 10^{-2}$	$l_e \leq -3.23 \times 10^{-2}$
(vi)	$l_e \leq -1.20 \times 10^{-1}$	$l_e \geq 1.02 \times 10^{-1}$
(vii)	$l_e \leq -1.14 \times 10^{-1}$	$l_e \geq 9.43 \times 10^{-2}$

TABLE I. Values of the lepton flavour asymmetry for which either the u (left column) or the d quark (right column) experiences a first-order transition.

the equilibrated case (i) we see that l has to be larger than allowed by observations of the CMB [37] and primordial element abundances [36]. We therefore conclude that in case of equal lepton flavour asymmetries a first-order QCD transition is excluded. On the other hand, scenarios (ii)-(vii) are by construction always compatible with CMB and BBN constraints and except for case (iv) all allow a first-order transition. It is also interesting to compare tab. I to the findings of [14] where scenarios (i) and (ii) were studied and to [10] where a more general version of scenario (v) was investigated ($|l_e + l_\mu| = -|l_\tau|$). The values for l_α rendering a first-order transition in tab. I are remarkably close to the maximal values ensuring the reliability of the Taylor expansion in [14], namely $|l_\mu| \leq 4 \times 10^{-2}$ (case (ii)) and $|l| \leq 7.5 \times 10^{-2}$ (case (i)). Furthermore, for scenarios (i) and (ii) the values in tab. I exceed the values for pion condensation, i.e. $|l| \geq 9 \times 10^{-2}$ (case (i)) and $|l_\mu| \geq 6 \times 10^{-2}$ (case (ii)) [14]. For scenario (v) they are only slightly smaller than what is needed to potentially form a pion condensate, i.e. $|l_e + l_\mu| > 1 \times 10^{-1}$ [10]. We therefore conclude that in case of a first-order cosmic QCD transition induced by large lepton asymmetries the formation of a pion condensate is also likely.

While table I already summarizes for which values of the lepton asymmetry a first-order QCD transition may occur, it is furthermore interesting to see how the cosmic trajectory looks like for such a first-order transition. Exemplarily we thereby focus on scenario (ii) and a first-order transition of the d quark. Fig. 2 shows the cosmic trajectory projected onto the (μ_B, T) -plane (top) and the net number density of the d quark for different values of the lepton flavour asymmetry l_μ . Observe the appearance of a kink in the trajectory (top) and a spike in the d quark net number density (bottom) for increasing values of $|l_\mu|$. This discontinuous feature reflects a first-order transition and arises for l_μ values between the green ($l_\mu = -6 \times 10^{-2}$) and the red curve ($l_\mu = -7 \times 10^{-2}$), confirming thereby the solution $l_\mu \leq -6.85 \times 10^{-2}$ given in tab. I.

Finally, let us compare the method introduced in this work to the method of [13, 14]. For this comparison we

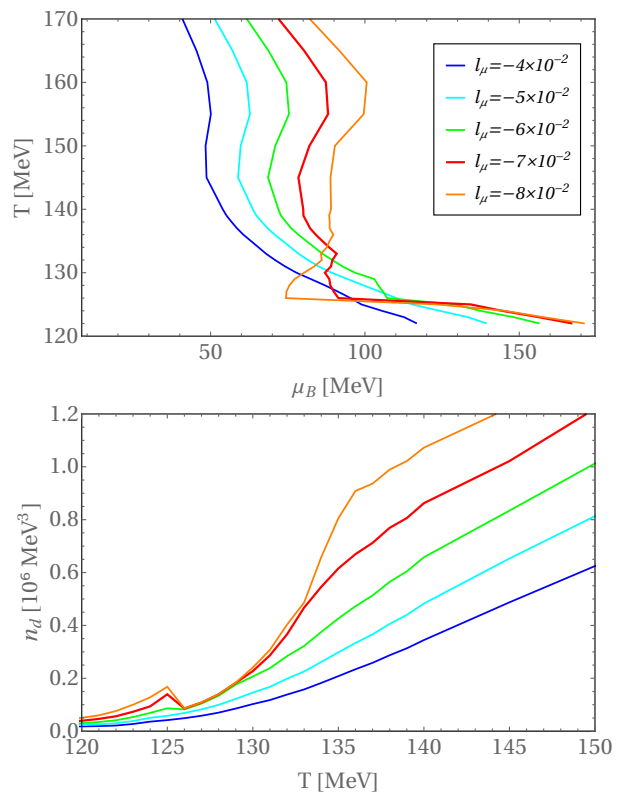


FIG. 2. Cosmic trajectory (top) and d quark number density (bottom) for scenario (ii), traversing a first-order QCD transition for increasing values of $|l_\mu|$.

focus on the case of equal lepton flavour asymmetries (i). In fig. 3 we show the cosmic trajectory derived by the method introduced in this work (solid lines) and by the method described in [14], where the dashed lines denote the high- and low-temperature regimes and \bullet symbols the results obtained by using lattice susceptibilities. The black line displays the standard trajectory, i.e. the trajectory assuming $l = -\frac{51}{28}b$. We see that at high temperatures our new method produces trajectories that are relatively similar to the ones obtained by [13, 14]. In the intermediate temperature regime the solid lines show the same trend as the dashed lines (i.e. the curves bending in the same direction) but the bending of the solid lines is much stronger. At low temperatures the standard trajectory converges to the HRG line relatively smoothly. However, for all larger l values instead of converging to the dashed HRG lines the solid lines rather overshoot. There are several possible reasons why the results of the two methods differ. First of all, as stated above, the RL truncation applied to derive the thermodynamic quantities in the QCD sector only allows to capture the main properties of the QCD phase structure but it is not expected to deliver exact results. The truncation can be systematically improved and in particular in [16, 32, 50] the CEP was estimated as $(T_{\text{CEP}}, \mu_{\text{CEP}})_{u/d} \simeq (110, 200)$

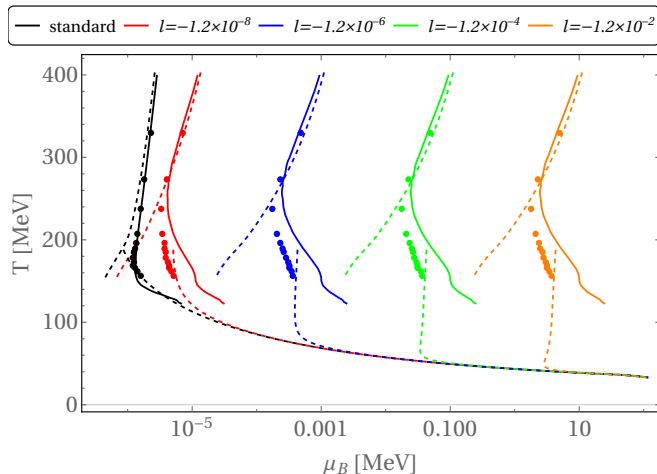


FIG. 3. Cosmic trajectory projected onto the (μ_B, T) -plane for equal lepton flavour asymmetries (case (i)) for different values of l , calculated with the method described in this work (solid lines) and with the method of [13, 14] (dashed lines, \bullet using lattice susceptibilities).

MeV. In the same manner also the solutions in tab. I are not expected to be exact but may be altered under these improvements. The computation of QCD thermal properties with the method of [16] is currently in progress and we hope to incorporate them into our method in a future study. Having said this, we also want to point out that the thermodynamic quantities as applied in the method of [13, 14] are as well not expected to be entirely definite. For example, in the intermediate temperature regime the quark number densities are built on the leading order of a Taylor expansion with lattice susceptibilities and are not yet continuum extrapolated. Furthermore, the perturbative QCD results for the thermodynamic quantities at zero chemical potential from [51] have been tuned to match the HRG model. Near the phase transition region the validity of the HRG model itself is however questionable.

Conclusions In this work, we incorporated the thermodynamic quantities of QCD matter derived from Dyson-Schwinger equations into calculations of the cosmic trajectory during the QCD epoch. Using the rainbow-ladder truncation as in [15] we calculated the net number and entropy densities of u/d, s and c quarks over a wide range of temperatures and chemical potentials. Following the idea of [12–14] we studied how the cosmic trajectory gets shifted towards larger chemical potentials when large lepton flavour asymmetries are assumed. Compared to the method of [13, 14] which is based on the application of lattice susceptibilities, our method shows good agreement at high temperatures but differences in the cosmic trajectories at temperatures $T \lesssim 260$ MeV. While we believe that these discrepancies are mainly due to the limitations from the rainbow-ladder truncation, our method nevertheless offers an up-to-now unique pos-

sibility to study the cosmic trajectory in a consistent way over a wide range of temperature and chemical potential and covering the main properties of QCD matter. In particular, for the first time our work revealed that large lepton flavour asymmetries can induce a first-order cosmic QCD transition. For equal lepton flavour asymmetries l_α this would require a total lepton asymmetry l that is already ruled out by observations of the CMB and primordial element abundances. If the individual lepton flavour asymmetries are varied a first-order transition is however feasible. Examples thereof are given by the cases (ii)-(vii) studied in this work and the corresponding values in tab. I. The new era of GW measurements therefore offers a way to not only study the QCD epoch but even to indirectly shed light on the origin of the matter-antimatter asymmetry of the Universe by constraining the lepton flavour asymmetries.

Acknowledgments We thank Dominik J. Schwarz, Dietrich Bödeker, Jan M. Pawłowski and Jürgen Schaffner-Bielich for interesting discussions and valuable comments. F. G. also thanks Dominik J. Schwarz and Dietrich Bödeker for invitation and hosting in Bielefeld University. I. M. O. acknowledges support by Fonds de la recherche scientifique (FRS-FNRS), as well as from the FPA2017-845438 and the Generalitat Valenciana under grant PROMETEOII/2017/033, and by the Deutsche Forschungsgemeinschaft (DFG) through the Grant No. CRC-TR 211. F. G. is supported by Alexander von Humboldt foundation.

* f.gao@thphys.uni-heidelberg.de

† isabel.oldengott@uclouvain.be

- [1] B. P. Abbott et al. (LIGO Scientific, Virgo), Phys. Rev. Lett. **116**, 061102 (2016), arXiv:1602.03837 [gr-qc].
- [2] J. Espinosa and M. Quiros, Phys. Lett. B **305**, 98 (1993), arXiv:hep-ph/9301285.
- [3] S. Iso, P. D. Serpico, and K. Shimada, Phys. Rev. Lett. **119**, 141301 (2017), arXiv:1704.04955 [hep-ph].
- [4] T. Hambye, A. Strumia, and D. Teresi, JHEP **08**, 188 (2018), arXiv:1805.01473 [hep-ph].
- [5] D. J. Schwarz, Annalen Phys. **12**, 220 (2003), arXiv:astro-ph/0303574 [astro-ph].
- [6] E. Witten, Phys. Rev. **D30**, 272 (1984).
- [7] K. Jedamzik, Phys. Rev. D **55**, 5871 (1997), arXiv:astro-ph/9605152.
- [8] K. Jedamzik and J. C. Niemeyer, Phys. Rev. D **59**, 124014 (1999), arXiv:astro-ph/9901293.
- [9] C. T. Byrnes, M. Hindmarsh, S. Young, and M. R. S. Hawkins, JCAP **08**, 041 (2018), arXiv:1801.06138 [astro-ph.CO].
- [10] V. Vovchenko, B. B. Brandt, F. Cuteri, G. Endrődi, F. Hajkarim, and J. Schaffner-Bielich, (2020), arXiv:2009.02309 [hep-ph].
- [11] D. Bödeker, F. Kühnel, I. M. Oldengott, and D. J. Schwarz, Phys. Rev. D **103**, 063506 (2021), arXiv:2011.07283 [astro-ph.CO].

- [12] M. Stuke, D. J. Schwarz, and G. Starkman, JCAP **1203**, 040 (2012), arXiv:1111.3954 [astro-ph.CO].
- [13] M. M. Wygas, I. M. Oldengott, D. Bödeker, and D. J. Schwarz, Phys. Rev. Lett. **121**, 201302 (2018), arXiv:1807.10815 [hep-ph].
- [14] M. M. Middeldorf-Wygas, I. M. Oldengott, D. Bödeker, and D. J. Schwarz, (2020), arXiv:2009.00036 [hep-ph].
- [15] F. Gao, J. Chen, Y.-X. Liu, S.-X. Qin, C. D. Roberts, and S. M. Schmidt, Phys. Rev. D **93**, 094019 (2016), arXiv:1507.00875 [nucl-th].
- [16] F. Gao and J. M. Pawlowski, (2020), arXiv:2010.13705 [hep-ph].
- [17] Y. Aoki, G. Endrodi, Z. Fodor, S. Katz, and K. Szabo, Nature **443**, 675 (2006), arXiv:hep-lat/0611014.
- [18] X. Luo and N. Xu, Nucl. Sci. Tech. **28**, 112 (2017), arXiv:1701.02105 [nucl-ex].
- [19] L. Adamczyk et al. (STAR), Phys. Rev. **C96**, 044904 (2017), arXiv:1701.07065 [nucl-ex].
- [20] A. Andronic, P. Braun-Munzinger, K. Redlich, and J. Stachel, Nature **561**, 321 (2018), arXiv:1710.09425 [nucl-th].
- [21] E. Shuryak, Rev. Mod. Phys. **89**, 035001 (2017), arXiv:1412.8393 [hep-ph].
- [22] F. Karsch, Nucl. Phys. A **698**, 199 (2002), arXiv:hep-ph/0103314.
- [23] S. Borsanyi, G. Endrodi, Z. Fodor, A. Jakovac, S. D. Katz, S. Krieg, C. Ratti, and K. K. Szabo, JHEP **11**, 077 (2010), arXiv:1007.2580 [hep-lat].
- [24] A. Bazavov et al. (HotQCD), Phys. Rev. D **90**, 094503 (2014), arXiv:1407.6387 [hep-lat].
- [25] D. Binosi and J. Papavassiliou, Phys. Rept. **479**, 1 (2009), arXiv:0909.2536 [hep-ph].
- [26] C. D. Roberts and S. M. Schmidt, Prog. Part. Nucl. Phys. **45**, S1 (2000), arXiv:nucl-th/0005064 [nucl-th].
- [27] G. Eichmann, H. Sanchis-Alepuz, R. Williams, R. Alkofer, and C. S. Fischer, Prog. Part. Nucl. Phys. **91**, 1 (2016), arXiv:1606.09602 [hep-ph].
- [28] C. S. Fischer, Prog. Part. Nucl. Phys. **105**, 1 (2019), arXiv:1810.12938 [hep-ph].
- [29] J. M. Pawlowski, Annals Phys. **322**, 2831 (2007), arXiv:hep-th/0512261.
- [30] N. Dupuis, L. Canet, A. Eichhorn, W. Metzner, J. M. Pawlowski, M. Tissier, and N. Wschebor, Phys. Rept. **910**, 1 (2021), arXiv:2006.04853 [cond-mat.stat-mech].
- [31] S.-x. Qin, L. Chang, H. Chen, Y.-x. Liu, and C. D. Roberts, Phys. Rev. Lett. **106**, 172301 (2011), arXiv:1011.2876 [nucl-th].
- [32] W.-j. Fu, J. M. Pawlowski, and F. Rennecke, Phys. Rev. D **101**, 054032 (2020), arXiv:1909.02991 [hep-ph].
- [33] F. Gao and J. M. Pawlowski, Phys. Rev. D **102**, 034027 (2020), arXiv:2002.07500 [hep-ph].
- [34] N. Aghanim et al. (Planck), arXiv: **1807.06209** (2018), arXiv:1807.06209 [astro-ph.CO].
- [35] E. W. Kolb and M. S. Turner, Ann. Rev. Nucl. Part. Sci. **33**, 645 (1983).
- [36] C. Pitrou, A. Coc, J.-P. Uzan, and E. Vangioni, Phys. Rept. **754**, 1 (2018), arXiv:1801.08023 [astro-ph.CO].
- [37] I. M. Oldengott and D. J. Schwarz, EPL **119**, 29001 (2017), arXiv:1706.01705 [astro-ph.CO].
- [38] S. Eijima and M. Shaposhnikov, Phys. Lett. **B771**, 288 (2017), arXiv:1703.06085 [hep-ph].
- [39] J. Ghiglieri and M. Laine, JHEP **02**, 014 (2019), arXiv:1811.01971 [hep-ph].
- [40] J. A. Harvey and E. W. Kolb, Phys. Rev. **D24**, 2090 (1981).
- [41] I. Affleck and M. Dine, Nucl. Phys. **B249**, 361 (1985).
- [42] Y. Y. Y. Wong, Phys. Rev. **D66**, 025015 (2002), arXiv:hep-ph/0203180 [hep-ph].
- [43] A. D. Dolgov, S. H. Hansen, S. Pastor, S. T. Petcov, G. G. Raffelt, and D. V. Semikoz, Nucl. Phys. **B632**, 363 (2002), arXiv:hep-ph/0201287 [hep-ph].
- [44] Note however that depending on the initial values and signs of l_α and depending on the mixing angles equilibration may however only be partial [52–54].
- [45] C. Caprini, S. Biller, and P. G. Ferreira, JCAP **0502**, 006 (2005), arXiv:hep-ph/0310066 [hep-ph].
- [46] The methods of [13] and [14] are identical, except for some improvements that are explained in [14].
- [47] P. Isserstedt, M. Buballa, C. S. Fischer, and P. J. Gunkel, Phys. Rev. **D100**, 074011 (2019), arXiv:1906.11644 [hep-ph].
- [48] P. Isserstedt, C. S. Fischer, and T. Steinert, Phys. Rev. D **103**, 054012 (2021), arXiv:2012.04991 [hep-ph].
- [49] O. Philipsen, Prog. Part. Nucl. Phys. **70**, 55 (2013), arXiv:1207.5999 [hep-lat].
- [50] P. J. Gunkel and C. S. Fischer, (2021), arXiv:2106.08356 [hep-ph].
- [51] M. Laine and Y. Schroder, Phys. Rev. **D73**, 085009 (2006), arXiv:hep-ph/0603048 [hep-ph].
- [52] S. Pastor, T. Pinto, and G. G. Raffelt, Phys. Rev. Lett. **102**, 241302 (2009), arXiv:0808.3137 [astro-ph].
- [53] G. Barenboim and W.-I. Park, JCAP **1704**, 048 (2017), arXiv:1703.08258 [hep-ph].
- [54] L. Johns, M. Mina, V. Cirigliano, M. W. Paris, and G. M. Fuller, Phys. Rev. **D94**, 083505 (2016), arXiv:1608.01336 [hep-ph].